

Thermal behavior of polarized Pd/D electrodes prepared by co-deposition

S. Szpak^a, P.A. Mosier-Boss^{a,*}, M.H. Miles^b, M. Fleischmann^c

^a SPAWAR Systems Center San Diego, Code 2636, 53560 Hull Street, San Diego, CA 92152-5001, USA

^b Department of Chemistry, Bates College, Lewiston, ME 04240, USA

^c Ente Nazionale Energie Alternative, Frascati, Italy

Received 16 December 2002; received in revised form 24 June 2003; accepted 16 July 2003

Abstract

Thermal behavior of polarized Pd/D electrode, prepared by the co-deposition technique, serving as a cathode in the Dewar-type electrochemical cell/calorimeter is examined. It is shown that: (i) excess enthalpy is generated during and after the completion of the co-deposition process; (ii) rates of excess enthalpy generation are somewhat higher than when Pd wires or other forms of Pd electrodes are used; (iii) positive feedback and heat-after-death effects were observed; and (iv) rates of excess power generation were found to increase with an increase in both cell current and cell temperature, the latter being higher.

© 2003 Elsevier B.V. All rights reserved.

Keywords: Excess enthalpy generation; Positive feedback; Heat-after-death

1. Introduction

Calorimetry is the preferred method of analysis of the thermal behavior of electrochemical cells. It is noted that such studies provide the basis for the investigation of the thermal behavior of a wide range of reactions, especially irreversible processes, in particular, an excess enthalpy generation in the negatively polarized Pd/D electrodes, the Fleischmann–Pons (F–P) effect. In an attempt to confirm/reject the Fleischmann–Pons claims, a number of cells/calorimeters were used: isoperibolic, differential, flowing fluid and zero gradient of which isoperibolic calorimetry was introduced in three designs, viz. open cell with radiative heat transfer [1–5], open cell with conductive heat transfer and closed cell with conductive heat transfer.

The basis for calorimetric measurements is the conservation of mass and energy and thus it requires the knowledge of processes under consideration, the sequence of events, the construction of the apparatus as well as the experimental procedure employed. Consequently, the formulation of an accurate model of an experiment is essential in the study of

electrochemical calorimetry, in general, and the F–P effect, in particular.

In examining the thermal behavior of the Pd/D system prepared by the co-deposition technique [6], we considered not only excess enthalpy generation but also other aspects such as positive feedback and heat-after-death. It is clear that calorimetry can provide more information than just whether or not excess enthalpy is generated.

2. Background information

The reported excess enthalpy production, the F–P effect, was challenged on various grounds. In order to answer some of them and show that they do not apply to the present work, we provided the relevant background information.

2.1. The Pd/D co-deposition technique

The Pd/D co-deposition is a process where palladium and deuterium are simultaneously deposited onto non-absorbing metallic substrates, e.g. Au and Cu, at sufficiently negative potentials from electrolytes containing palladium salts dissolved in heavy water. Once the solution composition is specified, the surface morphology and bulk structure can be

* Corresponding author. Fax: +1-619-767-4339.

E-mail address: boss@spawar.navy.mil (P.A. Mosier-Boss).

Nomenclature

| | |
|----------------------|--|
| C_p | heat capacitance ($\text{J g}^{-1} \text{mol}^{-1} \text{K}^{-1}$) |
| $E_c(t)$ | cell voltage at time t (V) |
| E_{th} | thermoneutral potential at bath temperature (V) |
| F | Faraday constant ($\text{C g}^{-1} \text{mol}^{-1}$) |
| ΔH_{ev} | rate of evaporative cooling (W) |
| i | iteration number |
| I | cell current (A) |
| J | thermal flux (W) |
| k_R | effective heat transfer coefficient (W K^{-4}) |
| L | latent heat of evaporation ($\text{J g}^{-1} \text{mol}^{-1}$) |
| M | number of moles of D_2O at $t = 0$ |
| p | vapor pressure at the cell temperature (Pa) |
| p^* | atmospheric pressure (Pa) |
| $Q_f(t)$ | rate of excess enthalpy generation (W) |
| t | time (s) |
| ΔT | temperature difference between the cell and the water bath (K) |
| V | volume (m^3) |
| <i>Greek letters</i> | |
| β | dimensionless term in Eq. (A.1) |
| γ | current efficiency toward a given reaction |

controlled by the cell current, thus ensuring reproducibility since both the metallurgical and surface chemistry aspects, are repeatable.

Incidentally, the co-deposition technique is not the only method for charging the Pd lattice to high D/Pd atomic ratios. These high ratios can be obtained by charging from the gaseous phase at extremely high pressures. The advantages/disadvantages of the electrochemically and pressure driven charging has been discussed, among others, by Conway and Jerkiewicz [7].

2.2. Structure of, and the processes within, the electrolyte/electrode interphase

The complex structure of the Pd/D₂O interphase and the operating forces acting upon it during loading/unloading can be best visualized by considering the sequence of events taking place. Briefly, the relevant points are: (i) transport and reduction of D⁺ ions; (ii) deuterium is deposited onto the electrode surface by the Volmer path, and removed by the Heyrovsky–Horiuti and Tafel paths, and by absorption; and (iii) the absorbed deuterium undergoes ionization followed by transport (diffusion) into the bulk metal.

The layer separating the electrolyte and the metal bulk phases contains particles that interact with particles in neighboring phases. If the number of interacting particles is large comparing to the total number of particles, then this layer is defined as non-autonomous. Hence, the electrode/electrolyte

interphase can be viewed as an assembly of non-autonomous layers whose structure is determined by operating processes [8].

2.3. The D₂ + O₂ recombination reaction

Except for Joule heating, the exothermic absorption of deuterium and the F–P effect, no other heat sources are activated during the co-deposition process. The frequently cited D₂ + O₂ recombination reaction, as being responsible for excess enthalpy generation, is not supported by experiment (recombination of evolving gases yielded volumes that were better than 1.0% of those calculated assuming 100.0% Faradaic efficiency [9], or theoretical considerations [10]). And yet the notion that recombination is responsible for the excess enthalpy generation persists. For example, Shanahan [11] observed that the short-lived hot spots [12,13] support the recombination theory. In his view, to quote: “The infrared photography of Szpak et al. is supportive evidence of this, if one considers the oxidation in subsurface bubbles to be rapid, which should be true of D₂ + O₂ flames”. Such interpretation is, indeed, difficult to understand and therefore accept. As pointed out by Fleischmann and Pons [14], such “hot spots” would have an intensity of ca. 6 nW—hence, impossible to detect by IR camera.

2.4. The D⁺ in the Pd lattice

While the processes in the electrolyte phase up to and including adsorption are well known, those occurring on and after crossing the contact surface remain unclear, especially at high concentrations of absorbed deuterium. With this in mind, Fleischmann and co-workers [15] posed a number of questions among them: (i) what is the nature of species at high X ($X = [\text{D}]/[\text{Pd}]$); (ii) what is the dynamics of D while in the Pd lattice; and (iii) what is the structure of the system under conditions of high X ? These questions were reformulated and partially answered by Preparata [16] using quantum electrodynamics coherence in condensed matter reasoning. His conclusions, pertinent to the present work, at high X ($X > 0.7$) are: (i) the D⁺ species are highly mobile (diffusion coefficient as high as $10^{-3} \text{cm}^2 \text{s}^{-1}$ has been reported [17]); and (ii) the chemical potential of D⁺ in tetrahedral sites is more negative than that in octahedral sites. The consequence of the latter is the formation of the γ -phase.

2.5. Dewar-type calorimetry

An independent evaluation of the Dewar-type cells, used by Fleischmann and Pons (and also in this research), by Hansen and Melich [18] states that these cells are “easily capable of 1.0% accuracy”.

A Dewar-type electrochemical cell, shown in Fig. 1, exhibits the following characteristics:

- (i) at low to intermediate cell temperatures (20–60 °C), heat transfer from the cell is dominated by radiation

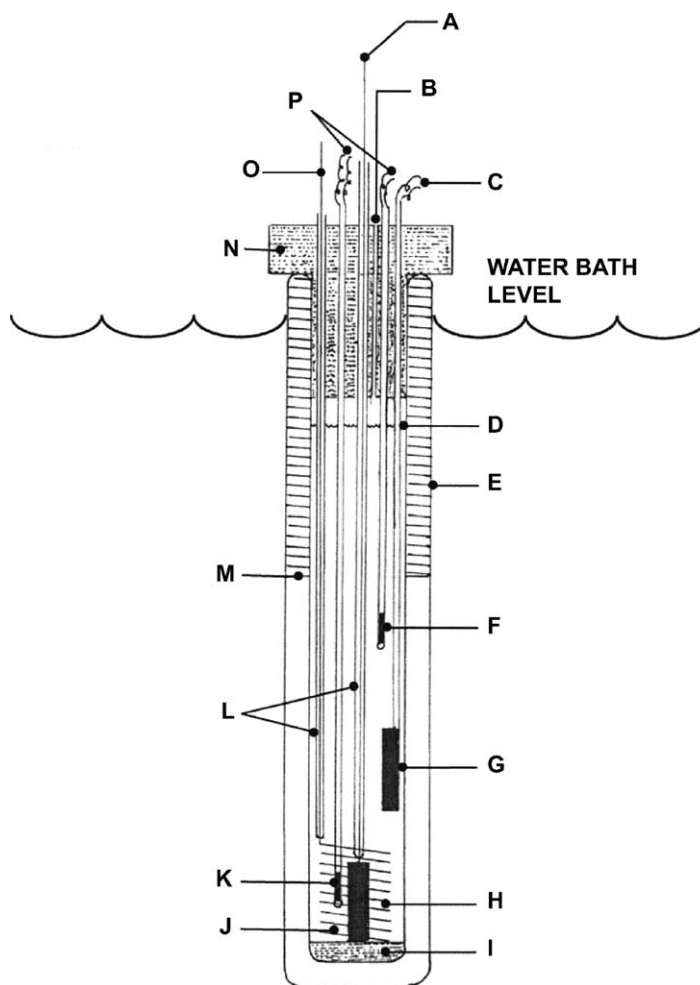


Fig. 1. The Dewar-type calorimeter used in this work: (A) cathode connection; (B) gas outlet; (C) heater connections; (D) electrolyte level; (E) silver mirror; (F) short termistor; (G) metal film resistor heater; (H) cathode; (I) Kel-F support plug; (J) anode; (K) long termistor; (L) capillary shields; (M) vacuum jacket; (N) Kel-F closure; (O) anode connection; (P) termistor connection.

- across the vacuum gap of the lower portion of Dewar vessel;
- (ii) the values of the heat transfer coefficient are close to those given by the product of the Stefan–Boltzmann coefficient and the radiant surface areas of the cells ($0.7 < 10^9 k_R < 0.76 \text{ W K}^{-4}$);
- (iii) the variation of the heat transfer coefficient with time (due to the progressive decrease in the level of electrolyte) may be neglected as long as the liquid level remains in the silvered portion (heat balance within 99.0%);
- (iv) at $I = 0.5 \text{ A}$ and $p = 101,325 \text{ Pa}$, the cooling due to evaporation is ca. 10% of that due to radiation;
- (v) measured uniformity of temperature of the electrolyte during cell operation is 0.02–0.3 s and somewhat more when resistive heater is employed;
- (vi) contribution of conduction is ca. 6.9%;
- (vii) relaxation time $\tau = C_p M^0 / 4k_R = 3600 \text{ s}$;
- (viii) mixing: radial, 3 s; axial, 20 s [19], i.e. cell behaves as a well-stirred tank;

- (ix) electrolyte volume (cell dimensions) selected so that the rate of change of the electrolyte temperature with enthalpy input is of 10 K W^{-1} .

3. Experimental

3.1. Experimental set-up

The experiment was carried out using an electrochemical system consisting of an Hi-Tek DT 2101 potentiostat/galvanostat. A separate potentiostat/galvanostat was used to deliver constant currents to the resistive heater used to calibrate the cells. The system was controlled by a 486 data acquisition computer which also controlled an Hewlett-Packard 44705A multiplexer and data acquisition system. This data acquisition system was on an IEEE–GPLB bus so that it would be anticipated that there would not have been any timing errors introduced into the measurements. Data were taken every 300 s.

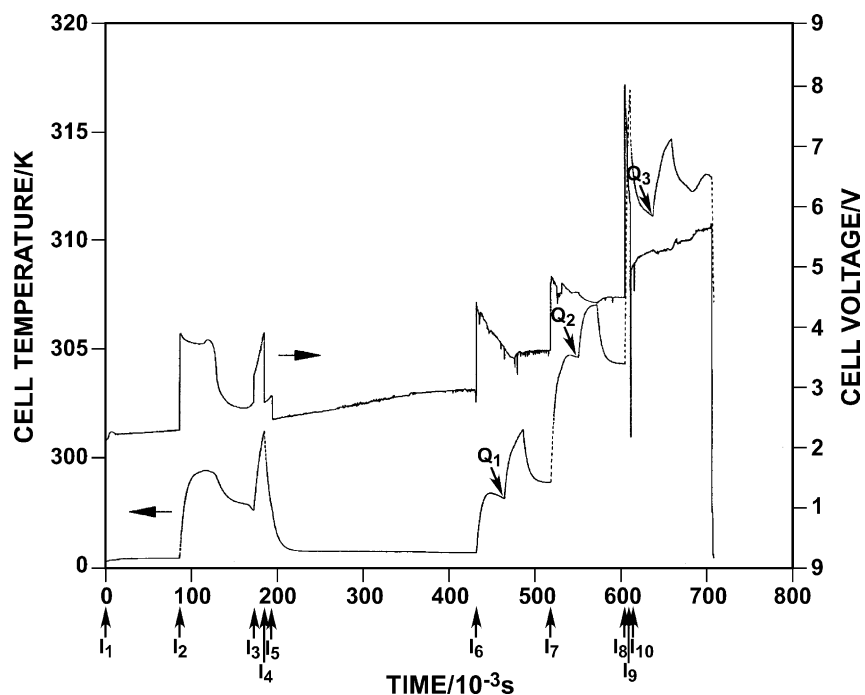


Fig. 2. Cell temperature, $T(t)$, and cell voltage, $E_c(t)$, as a function of time. Changes in the cell current at times indicated by arrows facing up. Resistive heater employed at times indicated by arrows facing down. Charging currents: $I_1 = 0.006$ A, $I_2 = 0.1$ A, $I_3 = 0.2$ A, $I_4 = 0.05$ A, $I_6 = 0.1$ A, $I_7 = 0.2$ A, $I_8 = 0.4$ A, $I_9 = 0.02$ A, $I_{10} = 0.3$ A. Calibration pulse: $Q_1 = Q_2 = Q_3 = 0.2500$ W.

The Dewar-type electrochemical cell was employed for the examination of the thermal behavior of the Pd/D system. A copper rod ($l = 2.5$ cm, $r = 0.2$ cm), upon which palladium and deuterium were co-deposited from a solution containing 0.025 M $\text{PdCl}_2 + 0.15$ M $\text{ND}_4\text{Cl} + 0.15$ M ND_4OD in D_2O (Isotec Inc., 99.9 at.% D) served as the negative electrode. Briefly, the co-deposition process (at $I = 0.006$ A) was completed in the first 24 h.

3.2. Data evaluation

Because the calorimetric equation is both non-linear and inhomogeneous, a number of simplifications must be made to provide a correct interpretation of thermal data and reach meaningful conclusions of a practical nature. Experience has shown that at low to intermediate temperatures, e.g. 20 – 60 °C, the behavior of a Dewar-type calorimeter is modeled adequately by the differential equation (cf. [Appendix A](#)

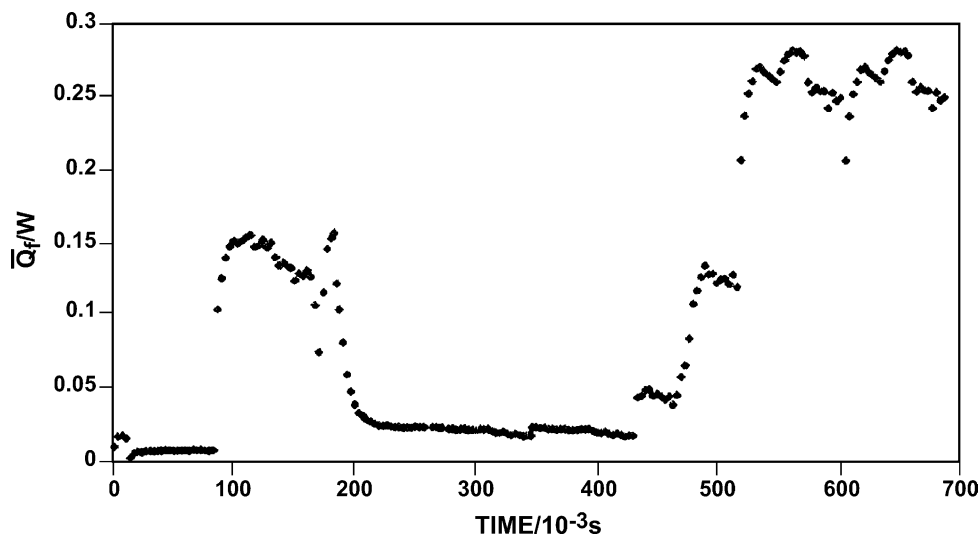


Fig. 3. Excess enthalpy generation, $\bar{Q}_f(t)$, as a function of time. Parameters used: $C_p M = 450$ J K $^{-1}$; $k_R = 0.85065$ W K $^{-4}$.

for a complete calorimetric equation):

$$C_p M \frac{dT}{dt} = (E_c - E_{th})I + Q_f(t) + Q_3 - \frac{3I}{4F} \left[\frac{p(t)}{p^* - p(t)} (C_{p,g} - C_{p,l}) \Delta T(t) + L \right] - k_R [(T_b + \Delta T(t))^4 - T_b^4]. \quad (1)$$

To measure the excess enthalpy generation, as indicated in Eq. (1), two parameters must be known, viz. the heat transfer coefficient, k_R and the water equivalent, $C_p M$. These parameters are inherently connected with the cell construction and experimental protocol, i.e. once determined for a given cell, they can be used for subsequent runs of the same cell. For the cell used in this research, the parameters are: $k_R = 0.85065 \times 10^{-9} \text{ W K}^{-4}$ and $C_p M = 450 \text{ J K}^{-1}$.

3.3. The $E_c(t)$ and $T(t)$ data

Since the evaluation is based on the examination of the cell voltage–time, $E_c(t)$, and cell temperature–time, $T(t)$, data in response to input enthalpies, $I(E_c - E_{th})$ and Q_3 , it was necessary to prescribe their time profiles in a manner yielding maximum information. Fig. 2 shows the $E_c(t)$ and $T(t)$ data due to the enthalpy inputs, $(E_c(t) - E_{th})I$, at times indicated by arrows facing upwards and by a resistive heater with $Q_3 = 0.2500 \text{ W}$ by arrows facing down. Briefly, three distinctly different time periods can be identified. The first period includes the co-deposition at 0.006 A, and charging at 0.1 A increased to 0.2 A and followed by a stepwise reduction to $I = 0.05$ and 0.02 A. The second time interval is the period of low charging rate ($I = 0.02 \text{ A}$) for ca. 72 h. The third time interval is characterized by drastic changes in cell operation—the cell current was increased/decreased in larger steps and, in addition, resistive heater was engaged at times indicated.

The $T(t)$ data are the normal, i.e. in the sense that an increase in the enthalpy input causes an increase in the cell temperature and vice versa. However, the examination of the $E_c(t)$ data reveals that there exist time periods when the cell temperature increases with decreases in the input enthalpy. As in the case of cells employing conventional electrodes, in this instance energy conservation requires the presence of additional (unidentified) heat sources.

4. Thermal effects

In an earlier communication [20], we have reported that in cells employing electrodes prepared by the co-deposition technique, excess enthalpy is generated reproducibly, at somewhat higher rates than on solid Pd electrodes and without the usual incubation period. Here, by examining the $T(t)$ data in conjunction with known enthalpy inputs,

we extend the analysis to include the “positive feedback” and the “heat-after-death”.

4.1. Excess enthalpy generation

Whether or not a particular cell generates excess enthalpy is determined by the energy and mass balance. Fig. 3 shows the 11-point average of the excess enthalpy generated, $\bar{Q}_f(t)$ whose integrated amount over the duration of this experiment was 75 kJ.

The comment has often been made that excess enthalpy generation can be explained by recombination of the electrically evolved gases. In this experiment, the total consumption of D_2O was 7.7 cm^3 instead of 7.2 cm^3 , assuming 100% Faradaic efficiency, which is within experimental error.

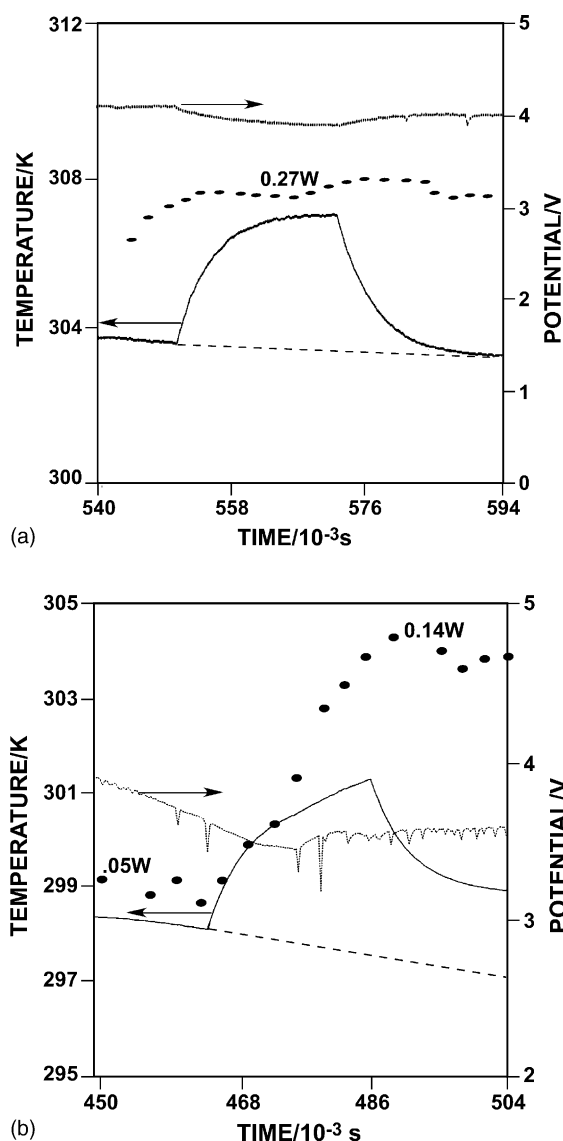


Fig. 4. The $E_c(t)$ and $T(t)$ curves following the application of calibration pulse: (a) at constant rate of excess enthalpy generation; (b) illustrating positive feedback.

Of special interest is the excess enthalpy generation during the co-deposition, i.e. at low current densities (e.g. as low as 6 mA cm^{-2}). Whether or not the excess heat observed in the course of co-deposition is due solely to exothermic absorption is difficult to ascertain because not much is known about the current efficiencies of the various operating reaction paths. More detailed calorimetry, beyond what was done in this experiment, would be required to assess the rate of excess enthalpy generation, if any. If, in fact, excess enthalpy is generated during the co-deposition period, it would have a profound influence on the understanding of its origin. However, making reasonable kinetic and thermodynamic assumptions together with high D/Pd atomic ratios of >1.0 within the Pd/D co-deposited films [21], one could conclude that an excess enthalpy generation cannot be excluded during the co-deposition process.

4.2. Effect of thermal perturbations—positive feedback

It is known that a perturbation of a system yields kinetic information through the examination of the $T(t)$ curves. Following the application of a calibration pulse, the $T(t)$ can be obtained by integration of Eq. (1). With constant E_c and Q_f , cell temperature, $T(t)$, increases exponentially and asymptotically approaches a new value. Upon cessation of the calibration pulse, cell temperature relaxes to a value that would have attained in the absence of the calibration pulse. A different behavior is expected for time-dependent cell voltage, $E_c(t)$, or variable rate of excess enthalpy generation, $Q_f(t)$.

During the experimental run, calibration pulses, Q_1 , Q_2 and Q_3 , were applied as indicated in Fig. 2. We selected for further discussion calibration pulses Q_1 and Q_2 representing different cell response to heat input. In one case, Fig. 4a, application of calibration pulse causes an exponential increase in cell temperature which, upon termination of calibration pulse, relaxes to the sloping temperature line. In-

spection of Fig. 2 shows that within the time period of temperature perturbation, the cell voltage remained constant (at $E_c = 4.0 \text{ V}$) indicating either no excess enthalpy generation or generation at a constant rate. Inspection of Fig. 3 shows the latter, i.e. generation at a constant rate of $Q_f = 0.24 \text{ W}$.

The cell response to the thermal input Q_1 , Fig. 4b, is different. Here, upon cessation of the thermal input, cell temperature does not relax to the expected value. Inspection of Figs. 2 and 3 reveals a time-dependent $E_c(t)$ and $Q_f(t)$, viz. decreasing E_c and increasing Q_f from 0.05 to 0.14 W. A positive feedback is apparent.

4.3. Effect of cell current perturbation—heat-after-death

A perturbation in cell current yields another characteristics of the Pd/D system, namely heat-after-death. At the beginning of the third day the charging current was increased to 0.2 A for a brief period of time, followed by a stepwise decrease to 0.05 A and finally to 0.02 A, which was maintained for the next ca. 72 h. The most important single result of this time period, viz. heat-after-death, is found in the analysis of the excess enthalpy decay following the stepwise reduction in the cell current. The decay of the six-point average, \bar{Q}_f , of \bar{Q}_f is shown in Fig. 5. In constructing this figure, it was assumed that the upper bound of any parasitic excess enthalpy generation due to the recombination is 0.009 W given by the last value of \bar{Q}_f at $t = 24 \text{ h}$, i.e. the values of \bar{Q}_f are the lower bound values. The detailed interpretation of the data requires the knowledge, at the very least, of the current efficiencies for the various reaction paths and the thermodynamics of the co-deposition process(es). However, it appears to us that if we make various plausible assumptions, then we must conclude that the Pd/D co-deposition is accompanied by excess enthalpy generation. Incidentally, some activity within the Pd/D films persisted long after termination of cell current [22].

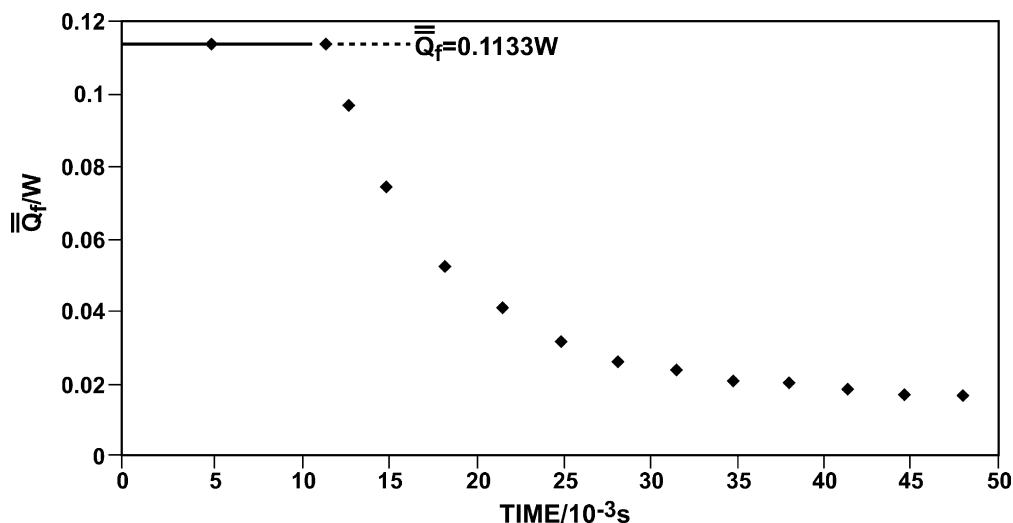


Fig. 5. The decay of $\bar{Q}_f(t)$ following the reduction in cell current (cf. Fig. 4) indicating the heat-after-death phenomenon.

5. Concluding remarks

In closing, we remark that results and conclusions of calorimetric measurement of the polarized Pd/D system are not limited to the excess enthalpy generation. Through the analysis of the effect of system's perturbation, both thermal and electrical, other characteristics can be displayed, e.g. positive feedback and heat-after-death.

Acknowledgements

The authors would like to thank Dr. F. Gordon for his interest and support.

Appendix A. Complete calorimetric equation

The complete calorimetric equation for the Dewar-type calorimeter is:

$$C_p M^0 \left[1 - \frac{(1 + \beta)\gamma I t}{2FM^0} \right] \frac{d\Delta T}{dt} - C_p \frac{(1 + \beta)I\Delta T}{2F} = \sum J_i, \quad i = 1, \dots, 6, \quad (\text{A.1})$$

where β is dimensionless term allowing for more rapid time-dependent decrease of water equivalent of cell than that expected from electrolysis alone and/or carried away in H_2 , O_2 gas bubbles; γ is the current efficiency and can be taken to be unity. The term $[1 - ((1 + \beta)It/2FM^0)]$ allows for change in the water equivalent, $C_p M^0$, with time.

The rates of enthalpy transfers are:

- $J_1 = (E_c(t) - E_{th})I$ is the enthalpy flow into the cell.
- $J_2 = Q_f(t)$ is the rate of excess heat generation within the Pd electrode and transferred into the electrolyte.
- J_3 is the known calibration heat source.
- $J_4 = -(\gamma I/F)[0.5C_{p,D_2} + 0.25C_{p,O_2} + 0.75(p/(p^* - p))C_{p,v}] + 0.75(\gamma I p L)/(p^* - p)$ is the enthalpy content of the gas stream.
- $J_5 = -k_R[1 - ((1 + \gamma)It/2FM^0)][(T_b + \Delta T)^4 - T_b^4]$ is a product of the time-dependent heat transfer coefficient and the effect of radiation. The parameter $\gamma = 1$ for cells operating at $0 < 60^\circ\text{C}$.
- $J_6 = (\gamma I/F) \int_0^t [0.5 + 0.75p/(p^* - p)] C_{p,1} \Delta T dt$ is the enthalpy input due to the addition of water to make up for the losses due to the electrolysis, $\gamma I/F$ and evaporation, $0.75p/(p^* - p)$.

The flow of cell current, I , produces changes in both the temperature and composition. Restricting our attention to

the electrolyte subsystem, there is an enthalpy gain within the Δt time period in the amount of $\int_{\Delta t} (E_c - E_{th})I dt$ (Joule heating) and the change in the mole numbers, n_k , due to the charge transfer reactions and evaporation, J_6 . The effect of β on $Q_f(t)$ can be neglected if the cells operate at $T < 60^\circ\text{C}$.

References

- [1] S. Pons, M. Fleischmann, Calorimetry of the Pd–D system, in: Proceedings of the First International Conference on Cold Fusion (ICCF-1), 1990, p. 1.
- [2] S. Pons, M. Fleischmann, The calorimetry of electrode reactions and measurements of excess enthalpy generation in the electrolysis of D_2O using Pd based cathodes, in: Proceedings of the Second International Conference on Cold Fusion (ICCF-2), 1991, p. 349.
- [3] M. Fleischmann, S. Pons, Calorimetry of the Pd/D system: from simplicity via complications to simplicity, in: Proceedings of the Third International Conference on Cold Fusion (ICCF-3), 1992, p. 47.
- [4] M. Fleischmann, S. Pons, M. LeRoux, J. Roulette, Calorimetry of the Pd/ D_2O system: the search for simplicity and accuracy, in: Proceedings of the Fourth International Conference on Cold Fusion (ICCF-4), 1993, p. 323.
- [5] M. Fleischmann, Simulation of the electrochemical cell (ICARUS) calorimetry, in: Thermal and Nuclear Aspects of the Pd/ D_2O system, vol. 2, Technical Report 1862, February 2002.
- [6] S. Szpak, P.A. Mosier-Boss, J.J. Smith, *J. Electroanal. Chem.* 302 (1991) 255.
- [7] B.E. Conway, G. Jerkiewicz, *Z. Phys. Chem.* 183 (1994) 1319.
- [8] R. Defay, I. Prigogine, A. Bellemans, *Surface Tension and Adsorption*, Longmans & Green, London, 1951.
- [9] S. Szpak, P.A. Mosier-Boss, R.D. Boss, J.J. Smith, *Fusion Technol.* 33 (1998) 38.
- [10] F. Will, *J. Electroanal. Chem.* 426 (1997) 177.
- [11] K.L. Shanahan, e-mail to M.A. Imam, 20 June 2002.
- [12] P.A. Mosier-Boss, S. Szpak, *Nuovo Cimento* 112A (1999) 577.
- [13] S. Szpak, P.A. Mosier-Boss, *Phys. Lett. A* 221 (1996) 141.
- [14] M. Fleischmann, S. Pons, *Phys. Lett. A* 187 (1994) 276.
- [15] C. Bartolomeo, M. Fleischmann, G. Larramone, S. Pons, J. Roulette, H. Sugiura, G. Preparata, *Trans. Fusion Technol.* 26 (1994) 23.
- [16] G. Preparata, *Trans. Fusion Technol.* 26 (1994) 397.
- [17] F. Celani, A. Spallone, P. Tripodi, D. Di Gioacchino, S. Pace, G. Salvaggi, P. Marini, V. DiStefano, M. Nakamura, A. Mancini, The effect of β – γ phase on H(D)/Pd overloading, in: Proceedings of the Seventh International Conference on Cold Fusion (ICCF-7), 1996, p. 62.
- [18] W.N. Hansen, M.E. Melich, *Trans. Fusion Technol.* 26 (1994) 355.
- [19] M. Fleischmann, S. Pons, M. LeRoux, J. Roulette, *Trans. Fusion Technol.* 26 (1994) 323.
- [20] S. Szpak, P.A. Mosier-Boss, M.H. Miles, *Fusion Technol.* 36 (1999) 234.
- [21] S. Szpak, P.A. Mosier-Boss, J.J. Smith, *J. Electroanal. Chem.* 379 (1994) 121.
- [22] J. Dea, P.A. Mosier-Boss, S. Szpak, Thermal and pressure gradients in polarized Pd/D systems, in: Proceedings of the Spring Meeting of the American Physical Society, Indianapolis, IN, 2002.